Journal of Biomedical Optics

BiomedicalOptics.SPIEDigitalLibrary.org

High-resolution handheld rigid endomicroscope based on full-field optical coherence tomography

Emilie Benoit a la Guillaume
Franck Martins
Claude Boccara
Fabrice Harms

SPIE.

High-resolution handheld rigid endomicroscope based on full-field optical coherence tomography

Emilie Benoit a la Guillaume,[a,*] Franck Martins,[a] Claude Boccara,[a,b] and Fabrice Harms[a]
[a]LLTech, Pépinière Paris Santé Cochin, 29 rue du Faubourg Saint-Jacques, 75014 Paris, France
[b]ESPCI ParisTech, PSL Research University, UMR 7587 CNRS, U979 INSERM, Institut Langevin, 1 rue Jussieu, 75005 Paris, France

Abstract. Full-field optical coherence tomography (FF-OCT) is a powerful tool for nondestructive assessment of biological tissue, i.e., for the structural examination of tissue in depth at a cellular resolution. Mostly known as a microscopy device for *ex vivo* analysis, FF-OCT has also been adapted to endoscopy setups since it shows good potential for *in situ* cancer diagnosis and biopsy guidance. Nevertheless, all the attempts to perform endoscopic FF-OCT imaging did not go beyond lab setups. We describe here, to the best of our knowledge, the first handheld FF-OCT endoscope based on a tandem interferometry assembly using incoherent illumination. A common-path passive imaging interferometer at the tip of an optical probe makes it robust and insensitive to environmental perturbations, and a low finesse Fabry–Perot processing interferometer guarantees a compact system. A good resolution (2.7 μm transverse and 6 μm axial) is maintained through the long distance, small diameter relay optics of the probe, and a good signal-to-noise ratio is achieved in a limited 100 ms acquisition time. High-resolution images and a movie of a rat brain slice have been recorded by moving the contact endoscope over the surface of the sample, allowing for tissue microscopic exploration at 20 μm under the surface. These promising *ex vivo* results open new perspectives for *in vivo* imaging of biological tissue, in particular, in the field of cancer and surgical margin assessment. © *2016 Society of Photo-Optical Instrumentation Engineers (SPIE)* [DOI: 10.1117/1.JBO.21.2.026005]

Keywords: endoscopy; endomicroscopy; full-field optical coherence tomography; tandem interferometry; medical and biomedical imaging; optical biopsy.

Paper 150630RR received Oct. 8, 2015; accepted for publication Jan. 13, 2016; published online Feb. 8, 2016.

1 Introduction

Optical endomicroscopy is an expanding field of research that consists of the integration of a high-resolution optical imaging technique into a small diameter probe in order to perform optical biopsies at the cellular level *in situ*. The development of these new technologies targets early cancer detection through a fast and minimally invasive process. Flexible endomicroscopes based on confocal microscopy and marketed by Mauna Kea Technologies are already used in gastroenterology, pulmonology, and urology medical departments in a few hundred hospitals in the world since they have demonstrated good accuracy in several clinical trials.[1–4] Developed more recently, spectrally encoded confocal microscopy (SECM)[5] has the potential to overcome two significant limitations of conventional confocal microscopy, which are the need for a contrast agent (fluorescein) and the small field of view (less than 500×500 μm^2). Based on endogenous reflectance, SECM acquires multiple points along a transverse line simultaneously, using spatial and spectral separation of light through the use of a grating. Thus, performing parallel acquisition releases the need for mechanical scanning in one direction and allows acquiring images at least three times faster than conventional confocal endomicroscopy with a system that fits into small diameter probes. For instance, Kang et al. demonstrated the imaging of 33 cm^2 of swine esophagus *in vivo* in 2 min using a 7-mm diameter SECM endoscopic probe.[6] Nonlinear endomicroscopy has also been developed in order to apply two-photon fluorescence (TPE) microscopy and second-harmonic generation (SHG) microscopy *in vivo*. Although its development has been slowed down, mainly by the high cost and bulky size of the light source, a high-sensitivity compact system was recently built and gave TPE and SHG images of liver, skin, and retina without using any contrast agent.[7] The other main endomicroscopy technique is based on Fourier domain optical coherence tomography (FD-OCT) and is referred to as volumetric laser endomicroscopy. The imaging part of the OCT system is encapsulated either in an optomechanically engineered pill that is swallowed by the patient[8] or in a catheter that is introduced into the body through the classical endoscopy instrument channel and positioned against the imaged lumen by endoscopic guidance[9] or by inflation for balloon-based probes.[10,11] In its most common use in gastrointestinal examination, the imaging spot is helically scanned into the digestive tract so that thousands of A-scans are quickly recorded during one rotation, leading to possible three-dimensional (3-D) visualization of the volumetric data set. Preliminary clinical studies have already been conducted on human volunteers *in vivo* and demonstrated good adequacy between the OCT images and the gold standard histology.[8–10] A commercial system (NvisionVLE Imaging System, Bedford) has also been developed by NinePoint Medical.[11]

Despite the above-mentioned promising results, endomicroscopy still requires improvements to achieve widespread clinical adoption, which explains the thriving variety of newly created devices and prototypes. The main efforts are focused on enhancing

*Address all correspondence to: Emilie Benoit a la Guillaume, E-mail: ebenoit@lltech.fr

1083-3668/2016/$25.00 © 2016 SPIE

the image quality in terms of resolution and contrast, and decreasing the operation time. Moreover, the current challenge is to upgrade the systems working without exogenous contrast agents in order to minimize the regulatory issues linked to permitted dose limits, risk of allergy, etc., and to allow for easier access to the medical market. Among noninvasive optical biopsy techniques, full-field OCT (FF-OCT) is known to offer one of the best resolutions since it is able to catch details at micron resolution within the tissues in three dimensions. As a consequence, it is an interesting candidate for endomicroscopy, which is evidenced by the work that has already been done to transfer the FF-OCT technique from a microscope to an endoscope.[12,13] Latrive and Boccara[13] presented a new FF-OCT design based on the coupling of two interferometers and validated it by imaging biological tissues *ex vivo* and skin *in vivo*.

However a long integration time (1 s/image acquisition) was needed to ensure a good signal-to-noise ration (SNR) and the system was still too bulky for handheld use, so fast *in situ* imaging was not achievable. In this paper, we report significant performance improvements on the system described in Ref. 13 and a new instrumental design allowing for handheld use of a fast FF-OCT rigid endomicroscope. A movie obtained with this endoscope on a rat brain coronal slice is presented and compared to the images recorded with a standard FF-OCT microscope.

2 Materials and Methods

2.1 *Tandem Interferometry*

The conventional FF-OCT optical setup for microscopy is based on a Linnik interferometer.[14] When considering its implementation as an endoscope, constraints of miniaturization, stability and resistance to environmental perturbations impose to divert from the classical configuration toward a design where the most exposed part—the probe—is as passive as possible. To do so, a tandem interferometry system is used, composed of:

i. an "active" interferometer, called the processing interferometer, since it defines the imaging depth within the tissue and provides the path modulation usually found in time domain OCT to extract the useful signal from the background;[14]
ii. a common-path "passive" interferometer, called the imaging interferometer, located at the distal end of the optical probe. It is a simple Fizeau interferometer defined by the partially reflective contact window and the imaging plane.

The idea of cascading two interferometers was introduced in fiber-coupled low-coherence interferometry to prevent signal loss induced by polarization mismatch between the reference and signal beams.[15,16] In the present endoscopy configuration, the reference beam is the light back-reflected by the window at the tip of the probe and the signal beam is the light back-reflected by the sample in contact with this window within a slice of thickness L_C, where L_C is the light source coherence length. The probe is thus insensitive to ambient perturbations since the two beams follow a common path through it. In the absence of a second interferometer, the maximum signal recorded would come from the slice of the sample in direct contact with the probe, corresponding to the zero path length difference. With the processing interferometer, a controlled path length difference is introduced, which needs to be compensated in the second interferometer so that the imaging plane is shifted further inside the sample.

2.2 *Full-Field Optical Coherence Tomography Endoscope*

Figure 1(a) gives an overview of the endoscope prototype optical design. As depicted in Fig. 1(b), the system presents a gun shape, where the grip carries the light source and associated optics, the barrel is the optical probe, and the back that supports the camera is the imaging arm. With a diameter of 5 cm and a length of 15 cm, the grip allows easy handling of the 1-kg total weight device. The 20 cm (length) × 5 mm (diameter) probe is long and thin enough to reach many of the endoscopic examination areas.

A high-power LED (M660L3, Thorlabs) is used as a low temporal and spatial light source ($\lambda_0 = 660$ nm, $\Delta\lambda = 25$ nm),

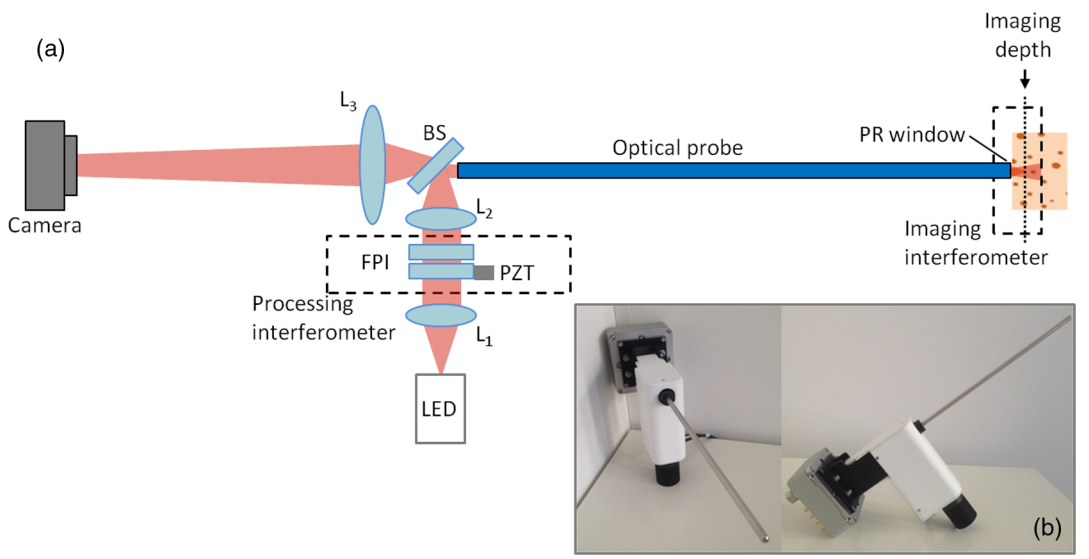

Fig. 1 (a) FF-OCT endoscope prototype setup and (b) pictures. L_1 – L_3, lenses; BS, beam splitter; FPI, Fabry–Perot interferometer; PZT, piezoelectric actuator; PR, partially reflective.

with a pair of lenses to conjugate the LED chip with the entrance of the optical probe (L1: 6-mm diameter, 21-mm focal length; and L2: 9-mm diameter, 22-mm focal length). The processing interferometer is positioned between the two conjugation lenses, where the light is collimated. After passing the processing interferometer, the light is reflected by a beam splitter plate before being injected into the optical probe so that 50% of the light power is lost and another 50% of the signal power is lost on its way back to the camera. Contrary to conventional medical endoscopes with peripheral illumination and central signal collection, the beam splitter plate is crossed both by the injected light emitted by the LED source and by the light coming from the sample, which explains such a significant power loss and the need for a high-power light source. The optical power delivered to the sample is 1mW. The probe is composed of a 20-cm long pitch 2 relay gradient index (GRIN) lens (GRINTECH, Germany) showing a diameter of 2 mm and a relatively small numerical aperture of 0.11 for image transfer, and of an objective lens (49271, Edmund Optics) with a focal length of 6 mm and a higher numerical aperture of 0.17 in order to ensure good lateral resolution. The probe ends with a planar partially reflective window (thickness 0.3 mm, diameter 2 mm) in order to create a surface where a plane contact is established with the tissue and where the reference wave originates. When in contact with biological tissue, the distal window reflects 8% of the incident light. This reference beam, as well as the signal beam coming from the imaging plane, which is the focal plane of the objective lens, travel back through the probe and are transmitted through the beam splitter plate, then conjugated with the camera (1440×1440 pixels, 12 μm pixel side, 700 Hz maximum frame rate, 2 million electrons full well capacity, Adimec, the Netherlands) thanks to an achromatic doublet lens of focal length 75 mm and diameter 15 mm. The camera integrated in the FF-OCT endoscope is also a prototype, which has been developed jointly by CMOSIS (Belgium) and Adimec in the framework of the CAReIOCA European FP7 research project to meet the specific technical requirements of FF-OCT in terms of full well capacity and speed. Internal mechanical mounting elements are custom-made in order to minimize space loss. An external protective housing is made from light and thin plastics to reduce weight. Custom-made Labview software is used to control the instrument and the acquisition. In particular, the software synchronizes the camera triggering with the movement of the piezoelectric actuator located on the processing interferometer in order to perform phase shifting OCT detection.

2.3 *Processing Interferometer*

In previous realizations of FF-OCT endoscopic setups using tandem interferometry, the processing interferometer is a Michelson-type one.[12,13] Because it is bulky, it has to be separated from the imaging probe in order to optimize the access possibilities of the device. This leads to the use of a multimode fiber to prolong the optical path between the two interferometers, which increases alignment issues and enhances the critical aspect of good parallelism tuning of the first interferometer. In our system, a low finesse, tunable Fabry–Perot interferometer is used (labeled FPI in Fig. 1) and easily inserted after the source and its collimating lens. Composed of two 50:50 plate beam splitters of diameter 12.5 mm, one of them being attached to a piezoelectric actuator (PA 8/14, Piezosystem Jena, Germany), the Fabry–Perot interferometer extends on 25 mm only in the direction of light propagation and presents a section of 35 mm $\times$ 45 mm transversally. The thickness of the air space between the two plates is precisely defined and controlled through the measurement of the fringes period with a spectrometer before integration into the endoscope. The thickness e determines the depth of the slice imaged with the FF-OCT device, which is equal to e/n, where n is the optical index of the sample (average 1.38 for biological tissue).

By changing the piezoelectric actuator offset voltage, the thickness of the Fabry–Perot interferometer can be modified, thus making it possible to scan the imaging plane through the sample depth and retrieve 3-D information. However, the depth of imaging is limited to the depth of focus of the optical probe[13] defined by the objective lens and the wavelength used, here set at 50 μm. For this first prototype endoscope, we did not include an axial scanning option, and the position of the imaging plane is fixed at 20 μm behind the surface of the tissue thanks to the Fabry–Perot interferometer thickness being tuned to 28 μm (fringes period of 7.5 nm). The piezoelectric actuator thus only provides the low amplitude modulation (3.5 V_{PP}) needed to introduce a π phase shift during one image acquisition in two. The displayed OCT signal is the difference between two consecutive images.

2.4 *Performance*

The main characteristics and performance of the endoscope are summarized in Table 1. The transverse resolution and the field of view are measured experimentally by imaging a high-resolution 1951 USAF target, and the axial resolution is also experimentally evaluated by translating a mirror through the depth of focus and measuring the full width at half maximum of the fringe envelope. Compared to the system presented in Ref. 13, the transverse resolution evaluated at 2.7 μm is better with this endoscope thanks to the improvement of the numerical aperture of the distal optics, but the axial resolution of 6 μm is poorer because of the spectrum of the light source. It was decided for the light source to prioritize optical power over spectral width so that the imaging speed is higher (to minimize the influence of movements), but the axial resolution is altered. Moreover, this sectioning ability of 6 μm stays close to the typical thickness of histology slides, typically 4 μm.

The detection sensitivity is affected by the tandem interferometry configuration, as explained in Ref. 16. As a consequence, a

Table 1 FF-OCT endoscope prototype technical data.

Dimensions	80 mm $\times$ 165 mm $\times$ 350 mm
Weight	1 kg
Probe length	195 mm
Probe diameter	5 mm
Axial resolution	6 μm
Transverse resolution	2.7 μm
Field of view	Circular, diameter 1.1 mm
Imaging depth	20 μm
Frame rate	1 to 10 Hz depending on the sample and the required averaging

6-dB (four-fold) decrease in the SNR is theoretically expected in comparison with the traditional single Linnik interferometer.[16] In order to evaluate the SNR loss in practice, a rat brain slice fixed in formalin is imaged *ex vivo* in several areas consecutively with the endoscope and with the LLTech commercial FF-OCT microscope (Light-CT scanner). All the experiments reported in this paper followed European Union and institutional guidelines for the care and use of laboratory animals. For the purposes of this comparative study as well as to evaluate the performance enhancement brought by the new camera, the endoscope is tested either with the Adimec camera or with the so-called conventional camera (1024×1024 pixels, 10.6 μm pixel side, 140 Hz maximum frame rate, 0.2 million electrons full well capacity, Photon Focus, Switzerland), which is the camera classically used in FF-OCT setups. The result of the comparison on two different areas of the rat brain slice is given in Fig. 2. On the left, the images recorded with a Light-CT scanner are shown. In the middle and on the right, the images taken with the prototype endoscope equipped with the Adimec camera and with the conventional camera, respectively, are shown. The images have been resized and cut in order to limit the comparison to a common zone at a common scale. The conditions of illumination (camera saturated at 80%) and averaging (30 accumulations) during the acquisition are also the same for each device. A tolerance of about 10 μm should be considered regarding the adequacy of the imaging planes with the Light-CT scanner and the endoscope given that the axial resolution and the compression of the sample are not the same in the two experiments.

The experiment shows a three-fold (5 dB) decrease in the SNR between the microscope and the endoscope equipped with the same camera. The possible error of adequacy between the two imaging planes, the difference of slice thickness due to the difference of axial resolution, and the existence of larger speckle grains on the endoscopic images, which reduces the possibility of finding uniform areas where the SNR can be compared with the Light-CT scanner images, are the possible reasons the image quality loss is lower than theoretically expected. The sensitivity of -88 dB usually expected from the Light-CT scanner under 30 accumulations is thus reduced to -83 dB with the endoscope prototype. In spite of the SNR alteration, anatomical features such as axons and myelin fibers or bundles are easily recognized on the endoscopic images, which is an important pillar of the diagnostic.

When the endoscope is equipped with the Adimec camera instead of the conventional camera, the SNR measured on the images increases by a factor of 2.7. This enhancement is the consequence of a higher full well capacity, provided that the light power is enough to saturate the sensor pixel wells. As the theoretical gain factor in full well capacity between the two cameras is 10, the expected gain factor in SNR is 3.2, since the SNR is proportional to the square root of the full well capacity (shot noise limited acquisition). As the Adimec camera is a prototype, the gain in full well capacity may be reduced, which explains the difference between the measurement and the theory. Another way to increase the SNR of the OCT images is to average more. Following this strategy, seven times more accumulations are needed to reach the same image quality with the conventional camera. Consequently, the second advantage of the Adimec camera is that at a given SNR, the imaging speed is multiplied by 4.

3 Results

The same rat brain slice sample is scanned with the FF-OCT endoscope prototype equipped with the Adimec camera

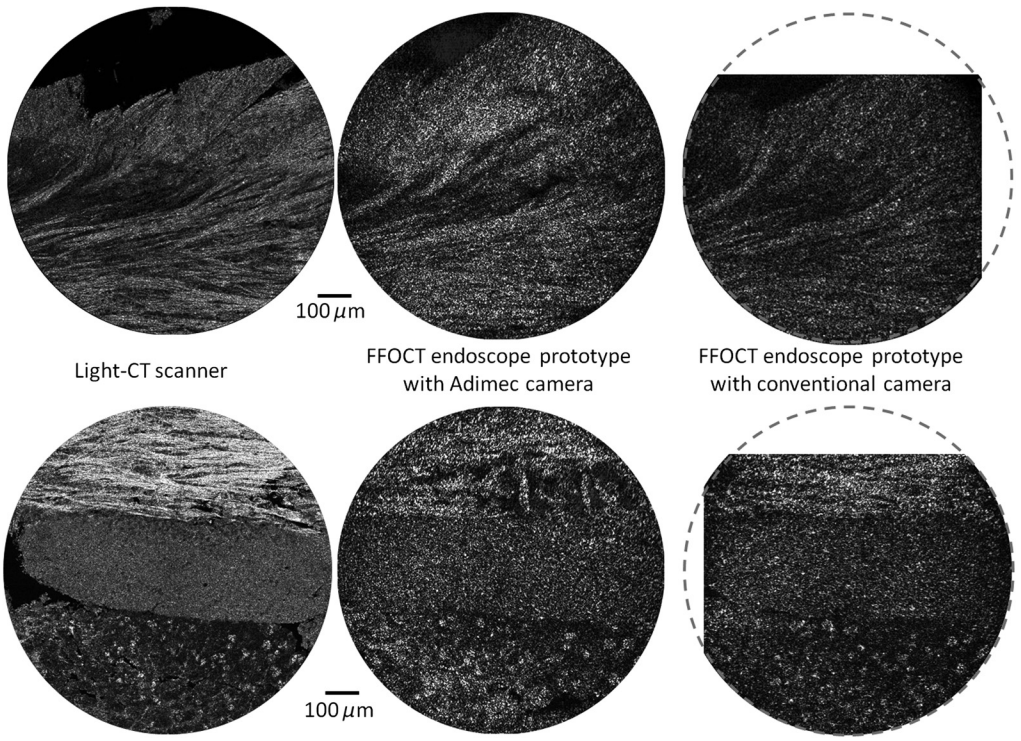

Fig. 2 Comparative study between (middle) FF-OCT images taken with the endoscope equipped with the Adimec camera or (right) with the conventional camera and (left) with the commercial Light-CT scanner. The sample is a rat brain coronal slice, imaged at 20 μm in depth with 30 averaging. The two rows correspond to two different areas of the sample.

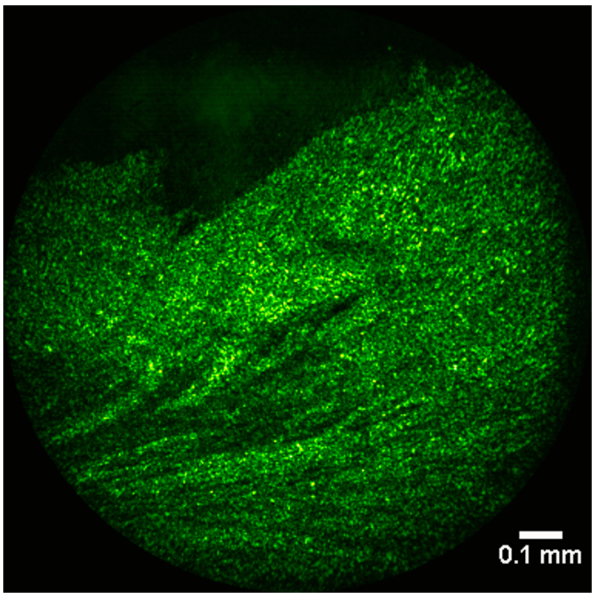

Fig. 3 Frame of Video 1 (QuickTime, 25 MB) showing rat brain slice imaging at 5 fps with the FF-OCT endoscope. [URL: http://dx.doi.org/10.1117/1.JBO.21.2.026005.1].

(Fig. 3). A "green hot" look-up table is chosen for the visualization of the series of images, since it improves visual perception of the contrast between the different structures. With 30 averaging/frame, the acquisition is done at 5 Hz. A wide-field image of the sample achieved with a Light-CT scanner is shown in Fig. 4 for comparison, where the path followed by the endoscope is notified by the dashed line. Several areas can be identified on the endoscopic movie depending on their structural architecture. The numbering of these areas is defined in Fig. 4. The axon fibers are easily recognized on the endoscopic movie with different orientations depending on their location inside the brain slice. In the areas labeled 1 and 5, the axon fibers are seen in a longitudinal view, whereas their cross-section is visible in area 3. Much thinner fibers of myelin also appear in areas 4 and 6. These smaller details are more easily caught when watching the images in motion than when looking at a static image taken with the endoscope.

4 Conclusion

In this paper, we presented, to the best of our knowledge, the first handheld FF-OCT endoscope. A tandem inteferometry design including a modulated Fabry–Perot etalon as the processing interferometer results in a compact and robust device. The high-resolution characteristics of FF-OCT are well preserved transversally thanks to the combination of a GRIN lens and an objective lens in the optical probe, slightly altered axially because of the use of a light source of smaller bandwidth. The movie recorded with this endoscope *ex vivo* on a rat brain slice shows a good level of structural detail at 20 μm within the sample after the surface of contact. Our current results suggest good expectactions for future *in vivo* experiments.

The comparison with the commercial FF-OCT microscope reveals some limitations of the endoscope that need to be pushed to reach the same image quality. Indeed, some further efforts can be made to get rid of the parasitic light coming from the several interface air/optical components crossed by the light injected into the sample, via the use of antireflective coatings and diaphragms, in order to increase SNR. Current developments also plan to allow new functionalities such as axial scanning of the sample. The diversity and the constant renewal of LED light sources commercially available also give the opportunity to improve the axial resolution of the system by increasing the spectral bandwidth and to obtain a higher speed gain by increasing the available light power. Finally, visualization and interpretation of FF-OCT images can also be improved through image processing, but this work should considerably benefit from the first users' feedback.

In the framework of the CAReIOCA project, the prototype endoscope was transferred to Gustave Roussy Institute (IGR) in Villejuif (France) in early June in order to be tested in a preclinical study on biopsy samples taken in the oral cavity (head, tongue, throat) from patients suspected for or diagnosed with head and neck cancer. About 50 samples are planned to be

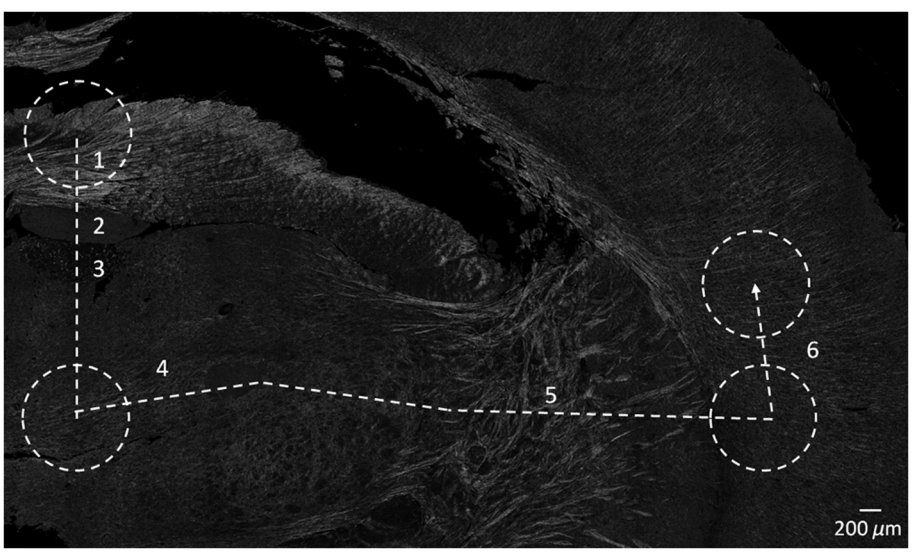

Fig. 4 Wide-field image (5×8.3 mm^2) of the coronal rat brain slice studied in Video 1 taken with a Light-CT scanner for comparison. The field of view and path of the endoscope are represented by the white dashed circles and arrow, respectively.

imaged. A preliminary work was done before to evaluate the potential of FF-OCT in the diagnosis of head and neck cancer. It consisted of the observation and analysis of biopsy samples with a Light-CT scanner by two pathologists after training, in comparison with the gold standard histology.[17] The diagnosis accuracy of the presence or not of a cancer reached 87%. The same pathologists are involved in the endoscopic study so that they are already familiar with FF-OCT images. The endoscopic movie review at IGR is still in progress and will result in the evaluation of the diagnostic capability of the FF-OCT endoscope prototype by the end of 2015. *In vivo* tests on an animal model will also give the opportunity to estimate the impact of the current speed limitations of the system and to appreciate the difficulty of maintaining the contact between the endoscope and the tissues despite the natural constraining movements and shapes of a living body. We believe that with further work on miniaturization and after the regulatory procedure is complete, the device will be ready for clinical evaluation in head and neck cancer diagnosis for biopsy guidance and margin assesment. Other diseases routinely diagnosed or monitored with rigid endoscopy are direct potential applications of FF-OCT endoscopy (e.g., arthroscopy), in particular where removal of tissue is of particular caution at a microscopic scale (neurosurgery). The introduction of FF-OCT endoscopy in standard medical procedures could give access to this microscopic view with minimal invasion and without any contrast agent.

Acknowledgments

We would like to thank LLTech's partners in the CAReIOCA project. This research was part of the CAReIOCA project and was supported by the European Union Seventh Framework Program FP7-ICT-2011-8 under Grant Agreement No. 318729 (www.careioca.eu).

References

1. M. Giovannini et al., "Results of a phase I–II study on intraductal confocal microscopy in patients with common bile duct stenosis," *Surg. Endosc.* **25**(7), 2247–2253 (2011).
2. M. W. Shahid et al., "Diagnostic accuracy of probe-based confocal laser endomicroscopy in detecting residual colorectal neoplasia after EMR: a prospective study," *Gastrointest. Endosc.* **75**(3), 525–533 (2012).
3. S. P. Chen and J. C. Liao, "Confocal laser endomicroscopy of bladder and upper tract urothelial carcinoma: a new era of optical diagnosis?" *Curr. Urol. Rep.* **15**, 437 (2014).
4. T. Hassan et al., "A novel method for in vivo imaging of solitary lung nodules using navigational bronshoscopy and confocal laser microendoscopy," *Lung* **193**, 773–778 (2015).
5. G. J. Tearney, R. H. Webb, and B. E. Bouma, "Spectrally encoded confocal microscopy," *Opt. Lett.* **23**(15), 1152–1154 (1998).
6. D. Kang et al., "Comprehensive confocal endomicroscopy of the esophagus in vivo," *Endosc. Int. Open* **2**, E135–E140 (2014).
7. J. Liu et al., "Low cost and compact nonlinear (SHG/TPE) laser scanning endoscope for bio-medical application," *Proc. SPIE* **9304**, 93041K (2015).
8. M. J. Gora et al., "Tethered capsule endomicroscopy enables less invasive imaging of the gastrointestinal tract microstructure," *Nat. Med.* **19**(2), 238–241 (2013).
9. T.-H. Tsai et al., "Ultrahigh speed endoscopic optical coherence tomography for gastroenterology," *Biomed. Opt. Express* **5**(12), 4387–4404 (2014).
10. M. J. Suter et al., "Esophageal-guided biopsy with volumetric laser endomicroscopy and laser cautery marking: a pilot clinical study," *Gastrointest. Endosc.* **79**(6), 886–896 (2014).
11. H. C. Wolfsen et al., "Safety and feasibility of volumetric laser endomicroscopy in patients with Barrett's esophagus (with videos)," *Gastrointest. Endosc.* **82**(4), 631–640 (2015).
12. W. Y. Oh et al., "Spectrally-modulated full-field optical coherence microscopy for ultrahigh-resolution endoscopic imaging," *Opt. Express* **14**(19), 8675–8684 (2006).
13. A. Latrive and A. C. Boccara, "In vivo and in situ cellular imaging full-field optical coherence tomography with a rigid endoscopic probe," *Biomed. Opt. Express* **2**(10), 2897–2904 (2011).
14. A. Dubois et al., "High-resolution full-field optical coherence tomography with a Linnik microscope," *Appl. Opt.* **41**(4), 805–812 (2002).
15. K. Bamford et al., "Optical radar detection of precancerous bronchial tissue," *Lasers Med. Sci.* **15**(3), 188–194 (2000).
16. H. D. Ford et al., "Comparative signal-to-noise analysis of fibre-optic based optical coherence tomography systems," *J. Mod. Opt.* **52**(14), 1965–1979 (2005).
17. F. De Leeuw et al., "Full-field OCT for fast diagnostic of head and neck cancer," *Proc. SPIE* **9303**, 93031Z (2015).

Emilie Benoit a la Guillaume received her PhD degree in physics in 2013 from Pierre et Marie Curie University for the work she did on acousto-optic imaging. She then joined LLTech as a research and development project manager to work on the latest evolutions of full-field optical coherence tomography technique, such as endoscopy.

Franck Martins is the manufacturing manager of LLTech. He has 17 years of experience in the development of medical devices with a cutting-edge expertise in opto-mechanical design and fabrication processes, as well as in CE marking and regulatory affairs.

Claude Boccara is a former dean of research at ESPCI and has more than 300 scientific publications, 11 awards and H index 48. He was involved in light-matter interactions, introduced new instruments and methods mostly limited in their performances by physical laws such as new kind of microscopies to increase depth and lateral resolution. Recently, optical approaches to ultimate measurements have found new fields of application from optical detection of gravitational waves to imaging though scattering media.

Fabrice Harms is the former CTO of LLTech (until September 2015). He has 14 years of experience in biophotonics and biomedical fields, managing research and product development programs as well as building and leading teams. He holds a PhD in physics from Pierre et Marie Curie University and is among the inventors of 6 patents.